Communication

Reversible Holographic Grating Formation in Polymer Solutions

Benoit Loppinet, Elvira Somma, Nikos Vainos, and George Fytas

J. Am. Chem. Soc., **2005**, 127 (27), 9678-9679• DOI: 10.1021/ja0529790 • Publication Date (Web): 16 June 2005

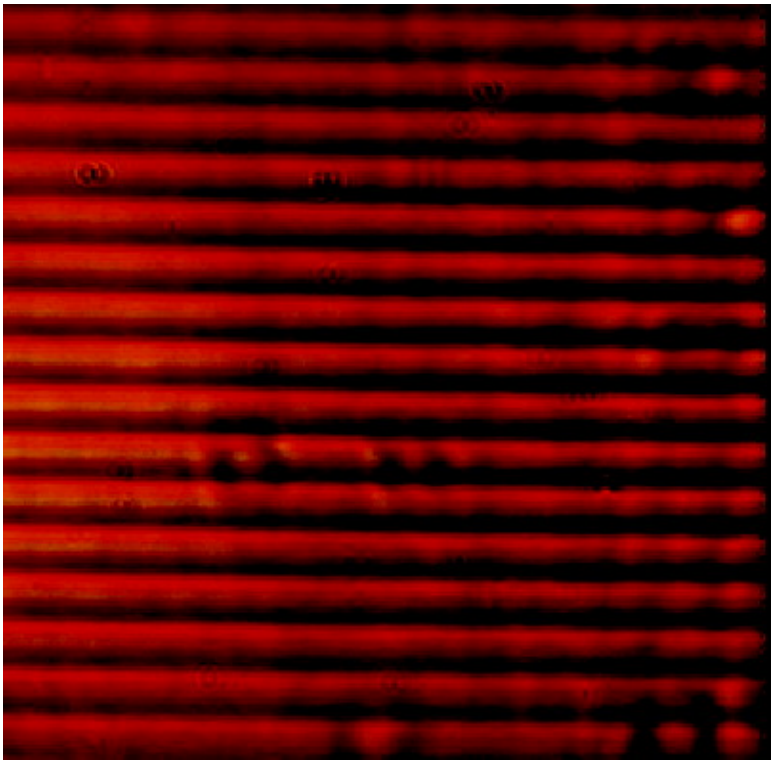

J|A|C|S
COMMUNICATIONS

Published on Web 06/16/2005

Reversible Holographic Grating Formation in Polymer Solutions

Benoit Loppinet,*,† Elvira Somma,† Nikos Vainos,‡,§ and George Fytas†,¶

F.O.R.T.H., Institute of Electronic Structure and Laser, P. O. Box 1527, 71110 Heraklion, Greece, NHRF-National Hellenic Research Foundation—Theoretical and Physical Chemistry Institute, 48 Vass. Constantinou Avenue, 11635 Athens, Greece, Department of Materials Science, University of Patras, Patras 26504, Greece, and Department of Materials Science and Technology, University of Crete, Heraklion 71103, Greece

Received May 6, 2005; E-mail: benoit@iesl.forth.gr

Optical radiation field gradients exert forces that are able to trap microscopic objects and immobilize them against Brownian motion.[1,2] Further to the established "optical tweezers" concepts that have opened the route to micromanipulation,[3] an unexpected light-induced material organization in fully transparent homogeneous polymer solutions was recently reported.[4] This phenomenon results in the formation of reversible string-like or dot-like micropatterns and appears totally unrelated to known photochemical or photophysical processes,[5,6] which alter locally the optical properties of a material.[5] Here, we demonstrate the reversible optical recording of holographic gratings in nonabsorbing solutions of common homopolymers. These phase gratings exhibit first-order diffraction efficiencies in excess of 50%. They are associated with the spatial modulation of the concentration of the polymer solute initiated, but not solely caused, by radiation forces.

The system used in these experiments consisted of entangled solutions of linear poly(isoprene-1,4) (PI) with a molecular mass of 963 kg/mol (or 14 160 monomer units per chain) in *n*-hexane at three concentrations (12.5, 13.3, and 16.5 wt %). The output of a continuous wave (cw) krypton ion laser emitting ~150 mW at $\lambda = 647$ nm divided into two beams of equal intensity (~20 mW/cm^2). The laser beams were incident and fully overlapped into a 50 mm × 2 mm × 10 mm glass cuvette containing the PI samples,[4] as shown in Figure 1, forming 9 mm thick gratings with wavevectors along the vertical direction (parallel to the 50 mm cuvette edge). Beam crossing (Bragg) angles were varied between 1.7 and 18.5°, respectively, resulting in interference gratings of spatial periods from 21 to 2 μm. A mechanical laser beam shutter and an optical power meter facilitating power measurements have also been used.

The laser-induced organization of the polymer solute leads to the formation of a periodic material pattern. The grating planes are viewed by the CCD camera along the direction perpendicular to the beam propagation axis (Figure 1, inset a). In the present case, this spatial modulation of polymer concentration is generated by the optical field gradient existent due to the periodic spatial modulation of the optical interference pattern. Further to the direct imaging, the holographic grating is monitored by the observed strong light diffraction responsible for the projected plots of Figure 1, inset b. Depending on the irradiating laser beam exposure (intensity by exposure time), the formed gratings depart from the linear unsaturated regime. Their profile tends to square, hence higher diffraction orders are observed (Figure 1b) and the pattern planes are becoming physically discrete.

The temporal evolution of the observed soft matter organization is studied by monitoring the diffraction efficiency of the holographic gratings. The first-order diffraction efficiency, $\eta \pm (t)$, of the grating

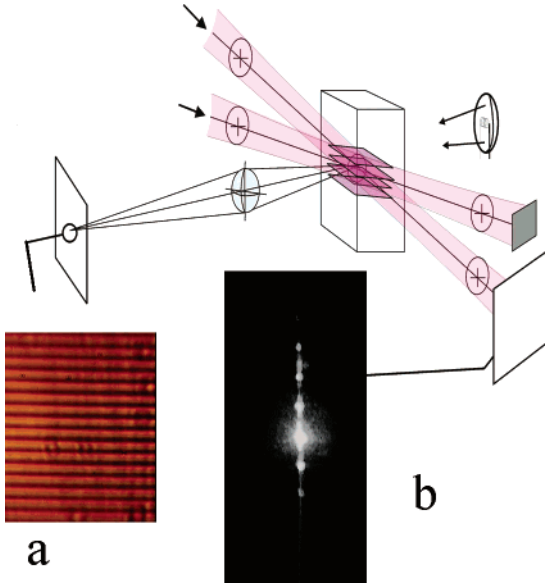

Figure 1. Schematic outline of the experimental configuration. The main beam of a red (647 nm) laser is divided into two beams, which fully overlap in the sample (S) forming the optical grating. A spatial periodic pattern corresponding to the grating planes is recorded by a microscope/CCD camera system (inset a). The projection of the diffracted beams on a screen is presented in inset b.

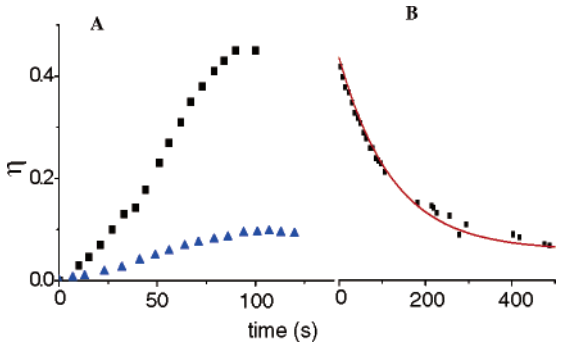

Figure 2. First-order diffraction efficiency recording (region A) for spatial periods of 21 μm (squares) and 2 μm (triangles), and the dark decay (region B) for spatial periods of 21 μm (following the recording displayed in A (square)). The line is an exponential decay, and the polymer concentration is about 12.5 wt %.

during typical recording (A) and decay (B) cycles is presented in Figure 2. In the recording phase, both laser beams are turned on to initiate pattern formation. Subsequently, one beam is shortly blocked at regular intervals in order to allow for detection of the diffracted part of the second writing beam during grating formation. The efficiency $\eta\pm$ is the ratio of the measured diffracted intensity to the incident intensity. In the present experimental conditions and

† F.O.R.T.H.
‡ NHRF.
§ University of Patras.
¶ University of Crete.

10.1021/ja0529790 CCC: $30.25

approaching saturation, $\eta \pm (t)$ exceeds 50% for a recording time of ~300 s. With the grating fully developed, numerous diffraction orders appear. The grating decays slowly in the dark. The diffraction efficiency is then recorded by turning on instantly one of the writing beams to detect its diffraction along the direction of the other beam. Grating decay is seen to be due to mass diffusion and/or mechanical motion and disorganization of the grating planes for the highly rigid patterns. Typical decay time constant under the present conditions is of the order of few hundreds of seconds.

By considering that grating formation is due to periodic polymer concentration variations in the illuminated region, the diffraction efficiency is $\eta \pm \sim \sin^2(\pi d\Delta n/\lambda \cos\theta)$ for a refractive index modulation Δn, grating thickness d, wavelength λ, and Bragg angle θ. In the present experimental conditions $\theta = 1.7°$, $d = 9$ mm, and thus $\Delta n \sim 10^{-5}$, suggesting a concentration modulation of $\Delta c = (dn/dc)^{-1}\Delta n \sim 4 \times 10^{-3}$ wt %. For comparison, the concentration fluctuations in the undisturbed semidilute polymer solution[8] are approximately 5 orders of magnitude smaller. On the basis of a purely electrostrictive mechanism in a liquid binary mixture, the expected concentration gradient for such laser-induced gratings is at least 3 orders of magnitude weaker.[7] Similarly, polarizability anisotropy along the chain backbone is found to be necessary but is not sufficient to provide a quantitative description of the phenomenon in terms of alignment mechanism. Gradient and alignment forces cannot solely account for the observed phenomenon; other collective effects such as chain connectivity certainly have to be included for a complete description.[4]

At a given laser intensity, the diffraction efficiency was found to increase with decreasing θ, that is, with decreasing spatial frequency of the illuminating interference pattern (Figure 2 region A). The lower concentration modulations for high spatial frequencies, despite higher field gradients, may well originate from mechanical disturbances inhibiting the full development of the anticipated diffracted efficiency. At spatial frequencies higher than ~500 mm^{-1} ($\theta > 9.5°$), recording efficiency becomes very weak. The intensity of the recording laser beams was found to be less critical in the operational limits set in these experiments, controlling solely the grating formation kinetics.

The concentration (refractive index) gratings fade out (Figure 2 region B) with a time scale depending on the spacing, the solution viscosity, and the exposure conditions and can, therefore, be controlled. When the recording is stopped in the early linear stage ($\eta < 0.05$), the characteristic decay time appears to scale with the square of the spacing. The inferred diffusion coefficient is orders of magnitude lower than the fast cooperative diffusion of semidilute polymer solutions and closer to the self-diffusion of polymer chain in entangled solutions.[9] For larger exposures, however, the decay mechanism appears to be more complex, in particular, with the occurrence of sedimentation.

Figure 2 shows reversible holographic gratings for the exemplar case of poly(isoprene-1,4) in *n*-hexane for two spatial frequencies. The observed high diffraction efficiencies verify the formation of high dielectric contrast grating patterns, which become mechanically rigid and long lived upon further optical exposure and/or for higher polymer concentrations. Further to the challenging fundamental research toward a deep understanding of the new phenomenon, an effectively giant electrostriction, these laser−matter interaction effects may open up new approaches in nanotechnology and photonics.

Acknowledgment. It is a pleasure to thank Dr. R. Sigel for his contribution at the initial stage of this work, and the GSRT of Greece for financial support.

References

(1) Ashkin, A.; Dziedzic, J. M.; Yamane, T. *Nature* **1987**, *330*, 769−771.
(2) Ashkin, A. *Proc. Natl. Acad. Sci. U.S.A.* **1997**, *94*, 4853−4860.
(3) MacDonald, M.; Spalding, G.; Dholakia, K. *Nature* **1999**, *426*, 810−813.
(4) Sigel, R.; Fytas, G.; Vainos, N.; Pispas, S.; Hadjichristidis, N. *Science* **2002**, *297*, 66−68.
(5) Juodkazis, S.; Mukai, R.; Yamaguchi, A.; Matsuo, S.; Misawa, H. *Nature* **2000**, *408*, 178−181.
(6) Olson, C. E.; Previte, M. J. R.; Fourkas, J. T. *Nat. Mater*. **2002**, *1*, 225−228.
(7) Tanaka, H.; Takagi, S. *J. Chem. Phys.* **2001**, *114*, 6286−6295.
(8) deGennes, P. G. *Scaling Concepts in Polymer Physics*; Cornell University Press: Ithaca, NY, 1979.
(9) Rauch, J.; Koehler, W. *Phys. Rev. Lett.* **2002**, *88*, 185901.

JA0529790